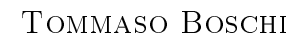
# MY SHITTY THESIS WITH MANY COMPLICATED AND INCONCLUSIVE PROJECTS THAT WILL END UP HAVING A LONG TITLE



 $31^{\rm st}$  March 2020

Submitted in partial fulfilment of the requirements of the Degree of Doctor of Philosophy

QUEEN MARY UNIVERSITY OF LONDON

Particle Physics Research Centre, School of Physics and Astronomy

and

University of Durham

Institute for Particle Physics Phenomneology

2

I, Tommaso Boschi, confirm that the research included within this thesis is my own work or that

where it has been carried out in collaboration with, or supported by others, that this is duly acknowl-

edged below and my contribution indicated. Previously published material is also acknowledged below.

I attest that I have exercised reasonable care to ensure that the work is original, and does not to the best

of my knowledge break any UK law, infringe any third party's copyright or other Intellectual Property

Right, or contain any confidential material.

I accept that the College has the right to use plagiarism detection software to check the electronic

version of the thesis.

I confirm that this thesis has not been previously submitted for the award of a degree by this or any

other university.

The copyright of this thesis rests with the author and no quotation from it or information derived from

it may be published without the prior written consent of the author.

Signature: Date:

Details of collaboration and publications:

#### Abstract

This is my thesis, get over with it.

# Contents

1	Neu	Neutrino physics in the Standard Model		
	1.1	Neutrino interactions	6	
	1.2	Neutrino detection	9	
		1.2.1 Water cherenkov	10	
		1.2.2 Gadolinium neutron capture	12	
	1.3	Neutrino Production	13	
<b>2</b>	Cha	apter 2	17	
3	Cha	apter 3	18	
A	Арр	pendix 1	19	
В	App	pendix 2	<b>2</b> 0	
$\mathbf{C}$	App	pendix 3	<b>2</b> 1	

## Neutrino physics in the Standard Model

The Standard Model (SM) is a gauge theory that describes the strong, electromagnetic, and weak interactions of elementary particles in the framework of quantum field theory. The theory is based on the local symmetry group

$$SU(3)_C \otimes SU(2)_L \otimes U(1)_Y$$
 (1.1)

where C, L and Y denote color, left-handed chirality and weak hypercharge, respectively. The gauge group uniquely determines the interactions and the number of vector gauge bosons that correspond to the generators of the group. They are eight massless gluons that mediate strong interactions, corresponding to the eight generators of  $SU(3)_C$ , and four gauge bosons, of which three are massive  $(W^{\pm}$  and Z) and one is massless, corresponding to the three generators of  $SU(2)_L$  and one generator of  $U(1)_Y$ , responsible for electroweak interactions. The symmetry group of the SM fixes the interactions, i.e. the number and properties of the vector gauge bosons, with only three independent unknown parameters: the three coupling constants of the  $SU(3)_C$ ,  $SU(2)_L$ , and  $U(1)_Y$  groups, all of which must be determined from experiments. On the contrary, the number and properties of scalar bosons and fermions are left unconstrained, except for the fact that they must transform according to the representations of the symmetry group, while the fermion representations must lead to the cancellation of quantum anomalies. The known elementary fermions are divided in two categories, quarks and leptons, according to the scheme:

Generation	1st	2nd	$3 \mathrm{rd}$
Quark	u	c	t
	d	s	b
Letpons	e	$\mu$	au
	$\nu_e$	$ u_{\mu}$	$ u_{ au}$

and their respective antiparticles. They are distinguished by the fact that quarks participate in all the interactions whereas leptons participate only in the electroweak interactions [?].

In the SM, electroweak interactions can be studied separately from strong interactions, because

the symmetry under the color group is unbroken and there is no mixing between the  $SU(3)_C$  and the  $SU(2)_L \otimes U(1)_Y$  sectors. On the other hand, the Glashow, Salam, and Weinberg theory well explains the group mixing between electromagnetic and weak interactions caused by a symmetry breaking process. This model and the discovery of the predicted W and Z bosons, in addition to the gluon, the top, and charm quarks, made the fortune of the Standard Model. Their redicted properties were experimentally confirmed with good precision and the recent discovery of the Higgs Boson [?] [?] is the last crowning achievement of SM.

Despite being the most successful theory of particle physics to date, the SM is actually limited in its approximation to reality, in that some clear evidences cannot be explained. The most outstanding breakthrough is the neutrino oscillations, which was awarded the Nobel Prize in Physics in 2015 and has proved that the neutrinos are not all massless, as it is assumed by theory. Mass terms for the neutrinos can be included in the SM, with the implications of theoretical problems. Likewise, the SM is unable to provide an explanation of the observed asymmetry between matter and anti-matter. It was noted by Sakharov that a solution to this puzzle would require some form of C and CP violation in the early Universe, along with Baryon number violation and out-of-equilibrium interactions. These facts suggest that the Standard Model is not a complete theory and additional physics Beyond the Standard Model (BSM) is required.

The study of neutrinos is for sure one of the most promising probe to BSM physics and is of vital importance to the future development of particle physics, in particular through precision measurement of their interactions. A deep understanding of neutrino interactions, and neutrino-nucleon interactions in particular, could lead to a great impact on long-baseline experiments, proton decay search, and supernova detection.

#### 1.1 Neutrino interactions

Neutrinos are colourless and chargless particles, thus sensitive only to weak interactions. Because of their nature, these leptons have small cross-sections and are difficult to measure. All the interactions are described by the the electroweak part of the SM, based on the symmetry group  $\mathrm{SU}(2)_L \otimes \mathrm{U}(1)_Y$ , and are governed by the lagrangian  $\mathcal{L} = \mathcal{L}^{(CC)} + \mathcal{L}^{(NC)}$ . In fact, neutrinos are mediated by the  $W^\pm$  for charged-current (CC) interactions and by the Z boson for neutral-current (NC) ones, whose respective lagrangians are:

$$\mathcal{L}^{(CC)} = -\frac{g}{2\sqrt{2}} \left( j_{W,L}^{\mu} W_{\mu} + \text{h.c.} \right)$$
 (1.2)

$$\mathcal{L}^{(NC)} = -\frac{g}{2\cos\theta_{\rm W}} j_{Z,\nu}^{\mu} Z_{\mu}, \qquad (1.3)$$

where the two currents are given by

$$j_{W,L}^{\mu} = 2 \sum_{\alpha = e, \mu, \tau} \overline{\nu_{\alpha L}} \gamma^{\mu} l_{\alpha L} \tag{1.4}$$

$$j_{Z,\nu}^{\mu} = \sum_{\alpha=e,\mu,\tau} \overline{\nu_{\alpha L}} \gamma^{\mu} \nu_{\alpha L} , \qquad (1.5)$$

and  $\vartheta_{\mathrm{W}} = 28.7^{\circ}$  is the Weinberg angle.

The easiest interaction that can be studied is the neutrino-electron elastic scattering

$$\nu_{\alpha} + e^{-} \rightarrow \nu_{\alpha} + e^{-} \,, \tag{1.6}$$

and its antineutrino counterpart<sup>1</sup>. For the electronic neutrino, both CC and NC interactions are allowed, while for  $\alpha = \mu, \tau$  the charged-current interactions are forbidden. The respective Feynman diagrams are shown in Fig. ?? and ??. For low neutrino energies, where the effects of the W and Z propagators can be neglected, the above processes are described by the effective charged-current and neutral-current lagrangians

$$\mathcal{L}_{\text{eff}}(\nu_e e^- \to \nu_e e^-) = -\frac{G_F}{\sqrt{2}} [\overline{\nu_e} \gamma^{\mu} (1 - \gamma^5) \nu_e] [\bar{e} \gamma_{\mu} ((1 + g_V^l) - (1 + g_A^l) \gamma^5) e]$$
 (1.7)

$$\mathcal{L}_{\text{eff}}(\nu_{\alpha}e^{-} \to \nu_{\alpha}e^{-}) = -\frac{G_{F}}{\sqrt{2}}[\overline{\nu_{\alpha}}\gamma^{\mu}(1-\gamma^{5})\nu_{\alpha}][\bar{e}\gamma_{\mu}(g_{V}^{l}-g_{A}^{l})\gamma^{5})e] \quad (\alpha = \mu, \tau).$$
 (1.8)

The differential cross-section with respect to the momentum transfer  $Q^2$ 

$$\frac{\mathrm{d}\sigma}{\mathrm{d}Q^2} = \frac{G_F^2}{\pi} \left[ g_1^2 + g_2^2 \left( 1 - \frac{Q^2}{2p_\nu \cdot p_e} \right)^2 - g_1 g_2 m_e^2 \frac{Q^2}{2(p_\nu \cdot p_e)^2} \right]. \tag{1.9}$$

The quantities  $g_1$  and  $g_2$  depend on the flavour of the neutrino and related to the vector and axial couplings,  $g_V$  and  $g_A$ . They are:

$$g_1^{\nu_e} = \frac{1}{2} + \sin^2 \theta_W \quad , \quad g_2^{\nu_e} = \sin^2 \theta_W$$
 (1.10)

$$g_1^{\nu_{\mu,\tau}} = -\frac{1}{2} + \sin^2 \vartheta_W \quad , \quad g_2^{\nu_{\mu,\tau}} = \sin^2 \vartheta_W \,.$$
 (1.11)

The differential cross-section as a function of the electron scattering angle in the laboratory frame is

$$\frac{d\sigma}{d\cos\theta} = \sigma_0 \frac{4E_{\nu}^2 (m_e + E_{\nu})^2 \cos\theta}{\left[ (m_e + E_{\nu})^2 - E_{\nu}^2 \cos^2\theta \right]^2} \left[ g_1^2 + g_2^2 \left( 1 - \frac{2m_e E_{\nu} \cos^2\theta}{(m_e + E_{\nu})^2 - E_{\nu}^2 \cos^2\theta} \right)^2 -g_1 g_2 \frac{2m_e^2 \cos^2\theta}{(m_e + E_{\nu})^2 - E_{\nu}^2 \cos^2\theta} \right],$$
(1.12)

where

$$\sigma_0 = \frac{2G_F^2 m_e^2}{\pi} \,. \tag{1.13}$$

For what concern the experiments, neutrino interactions with nucleons are easier to study thanks to the much larger cross-section and a more diverse range of processes, despite being less straightforward

 $<sup>^{1}</sup>$ In terms of Feynam diagrams, the t-channel diagram is replaced by the s-channel diagram.

to deal with theoretically. In general, these processes can be categorised according to the momentum transfer. At small  $Q^2$ , elastic interactions dominate and may be brought about by both charged and neutral currents. When this occurs via neutral currents, all flavour of neutrinos and anti-neutrinos can scatter off both neutrons and protons in what is referred to as "NC elastic" scattering. The process is:

$$\nu_l + N \to \nu_l + N, \bar{\nu}_l + N \to \bar{\nu}_l + N, \tag{1.14}$$

Once neutrinos acquire sufficient energy they can also undergo the analogous charged current interactions, called "quasi-elastic", due to the fact that the recoiling nucleon changes its charge and mass transfer occurs. The processes are

$$\nu_l + n \to p + l^- \tag{1.15}$$

$$\bar{\nu}_l + p \to n + l^+ \,, \tag{1.16}$$

with  $l = e, \mu, \tau$ . For the muonic neutrino with energy below one GeV, the CCQE is the dominant interaction, event though the cross-section plateaus at higher energies, as the available  $Q^2$  increases: it becomes increasingly unlikely for the nucleon to remain intact.

The physics behind the CC quasi-elastic processes is more complicated. The differential cross-section for the scattering in the laboratory frame is given by

$$\frac{\mathrm{d}\sigma_{CC}}{\mathrm{d}Q^2} = \frac{G_F^2 |V_{ud}|^2 m_N^4}{8\pi (p_\nu \cdot p_N)^2} \left[ A(Q^2) \pm B(Q^2) \frac{s - u}{m_N^2} + C(Q^2) \frac{(s - u)^2}{m_N^4} \right],\tag{1.17}$$

where the plus sign refers to the N=n interactions, while the minus sign to N=p.

$$\frac{\mathrm{d}\sigma_{CC}}{\mathrm{d}\cos\theta} = -\frac{G_F^2 |V_{ud}|^2 m_N^2}{4\pi} \frac{p_l}{E_\nu} \left[ A(Q^2) \pm B(Q^2) \frac{s-u}{m_N^2} + C(Q^2) \frac{(s-u)^2}{m_N^4} \right],\tag{1.18}$$

The functions  $A(Q^2)$ ,  $B(Q^2)$ , and  $C(Q^2)$  depends on the nucleon form-factors in the following way:

$$A = \frac{m_l^2 + Q^2}{m_N^2} \left\{ \left( 1 + \frac{Q^2}{4m_N^2} \right) G_A^2 - \left( 1 - \frac{Q^2}{4m_N^2} \right) \left( F_1^2 - \frac{Q^2}{4m_N^2} F_2^2 \right) + \frac{Q^2}{m_N^2} F_1 F_2 - \frac{m_l^2}{4m_N^2} \left[ (F_1 + F_2)^2 + (G_A + 2G_P)^2 - \frac{1}{4} \left( 1 + \frac{Q^2}{4m_N^2} \right) G_P^2 \right] \right\}$$

$$(1.19)$$

$$B = \frac{Q^2}{m_N^2} G_A(F_1 + F_2) \tag{1.20}$$

$$C = \frac{1}{4} \left( G_A^2 + F_1^2 + \frac{Q^2}{4m_N^2} F_2^2 \right). \tag{1.21}$$

The form factors  $F_1(Q^2)$ ,  $F_2(Q^2)$ ,  $G_A(Q^2)$ , and  $G_P(Q^2)$  are called, respectively, *Dirac*, *Pauli*, *axial*, and *pseudoscalar* weak charged-current form factors of the nucleon. These funtions of  $Q^2$  describe the spatial distributions of electric charge and current inside the nucleon and thus are intimately related to its internal structure.

CCQE interactions are particularly important to neutrino physics for mainly two reasons:

• measurements of the differential cross-section in Eq. 1.17 give information on the nucleon form-factors, which are difficult to measure;

• their nature as two-body interactions enable the kinematics to be completely reconstructed, and hence the initial neutrino energy determined which is critical for measuring the oscillation parameters.

In fact, if the target nucleon is at rest, at least compared to the neutrino energy, then this can be calculated as:

$$E_{\nu} = \frac{m_n E_l + \frac{1}{2} (m_p^2 - m_n^2 - m_l^2)}{m_n - E_l + p_l \cos \theta_l},$$
(1.22)

where the measurement of the momentum,  $p_l$  and the angle with respect to the neutrino,  $\theta_l$ , of the outgoing charged lepton are only required.

Similar calculations can be made for the NCQE scatterings. The cross-sections have the same form as the CC cross-sections in Eq. 1.17 and 1.18, without the mixing term  $|V_{ud}|^2$  and with the proper nucleon form factors. Since the values of the electromagnetic form factors,  $F_1$  and  $F_2$ , are reasonably well known and the part in Eq. 1.19 containing  $G_P$  can be often neglected, thanks to the different mass magnitudes of leptons and nucleons, the axial form factor,  $G_A$ , can be determined through measurements of the charged-current quasielastic scattering processes. On the contrary, measurements of the neutral-current elastic scattering cross-section give information on the *strange* form factors of the nucleon, whose main contribute comes from the strange quark.

The low  $Q^2$  region also presents an inelastic scattering contribution mostly affected by resonance production, where the nucleon is excited into a baryonic resonance before decaying. At high  $Q^2$ , inelastic scattering is dominated by deep inelastic scattering (DIS), because the neutrino can scatter directly off a constituent quark, fragmenting the original nucleon. In between these extreme scenarios, an additional contribution comes from interactions where the hadronic system is neither completely fragmented nor forms a recognisable resonance. These interactions are referred to as "shallow inelastic scattering", and there is no clear model for dealing with them.

#### 1.2 Neutrino detection

Being electrically neutral and uncoloured particles, neutrinos can only interact through weak interactions. For this reason, coupled with the small cross-sections typical of the weak force, the study of neutrino results in a challenging task. Direct observation is unfeasible, thus detection must rely on weak interactions with matter, where their SU(2) charged counterparts are either produced or scattered, by CC or NC interactions respectively. The physics is mediated by the lagrangians in Eq. 1.2 and 1.3.

Large active volumes have to be employed, such that a significant number of neutrino can be considered and interaction probability is thus increased. These apparatus are often built underground to shield the detector from cosmic rays and other barckground radiation. Apart from providing matter to interact with, at the same time these volumes must be capable of detecting the scattered charged

leptons. Many are the materials or substances that can be used, like chlorine, gallium, solid or liquid scintillators.

One of the most promising techniques is to combine liquid argon with time projection chambers. As with most other liquefied noble gases, argon has a high scintillation light yield (ca 51 photons/keV[arXiv:1004.0373]), is transparent to its own scintillation light, and is relatively easy to purify. Compared to xenon, argon is also cheaper and has a distinct scintillation time profile which allows the separation of electronic recoils from nuclear recoils.

A more dated and better-known technology is the *water Cherenkov* method, where the detector is used to record the Cherenkov light produced when the particles pass through pass through tanks full of purified water.

#### 1.2.1 Water cherenkov

The speed of light in vacuum is a universal constant, c, and it is a physical limit of the propagation of information, as stated by the special theory of Relativity. However, when in a medium, light may travel at speed significantly less than c. This reduction of speed depends on the relative permittivity,  $\varepsilon$ , of the material in which light is propagating. Because of the non-zero real part of the dielectric constant, the electromagnetic (EM) field is modified and the phase velocity of light changes into

$$v_P = \frac{c}{\sqrt{\varepsilon(\lambda)}} = \frac{c}{n(\lambda)},$$
 (1.23)

where  $n(\lambda) > 1$  is the refractive index of the medium and depends on the wavelenght (energy) of the wave.

A charged particles moving at a constant velocity in a dielectric medium disrupts the local electromagnetic field, by deforming its molecules and temporarily polarising the material. The dipoles are restored almost instantaneously and thus become impulsive sources of EM waves. If the velocity of the passing particle,  $v = \beta c$ , is less than the speed of the light in the medium as expressed in Eq. 1.23, i.e.  $\beta < 1/n$ , then the total energy flux of the excited field is zero and EM waves are not irradiated. On the contrary, if  $\beta > 1/n$ , the perturbance left by the passage of the particle is such that the energy is released coherently. The result is that the field is different from zero in a cone coaxial with respect to the direction of the charged particle, whose direction is opposite to the particle motion. As far as the photons are concerned, these are emitted coherently to a fixed angle with respect to the particle motion. With the help of Fig. ??, it is easy to find that:

$$\sin \alpha = \frac{1}{\beta n} \tag{1.24}$$

$$\cos \theta = \frac{1}{\beta n} \,. \tag{1.25}$$

where  $\alpha$  is the apex angle of the cone and  $\theta$  is the photon angle with respect to the particle direction.

For an ultra-relativistic particle, for which  $\beta \sim 1$ , there is a maximum angle of emission, given by:

$$\cos \theta_{\text{MAX}} = \frac{1}{n}. \tag{1.26}$$

The phenomenon is called *Cherenkov effect*, and it occurs everytime a charged particle passes through a dielectric medium at a speed:

$$\beta > \frac{1}{n} \,. \tag{1.27}$$

According to the theory of electromagnetic waves, a charged particle moving uniformly does not irradiate and this proves that the Cherenkov radiation is not related with Bremsstrahlung.

This condition can be expressed in terms of the particle energy, given that  $E^2 = p^2 + m^2$  and  $\beta = p/E^2$ . The threshold becomes:

$$\frac{E}{m} > \frac{1}{\sqrt{1 - 1/n^2}},$$
 (1.28)

with m the mass of the charged particle.

The radiation is emitted in the visible and near visible regions of the EM spectrum, for which n > 1. A real medium is always dispersive and radiation is restricted to those frequencies bands for which  $n(\nu) > \frac{1}{\beta}$ . In the x-ray region, for instance,  $n(\nu)$  is always less than one and radiation is forbidden at this energies, because Eq. 1.27 cannot be satisfied.

Truly, coherent emission of light needs two more conditions to be fulfilled:

- the length of the track of the particle in the medium should be large compared with the wavelength,
   λ, of the radiation in question, otherwise diffraction effects will become dominant;
- the velocity of the particle must be constant during its passage through the medium, or, to be more specific, the differences in the times for particle to traverse successive  $\lambda$  distances should be small compared with the period  $\frac{\lambda}{c}$  of the emitted light.

The number of photons emitted by a charged particle of charge Ze per unit path length and per unit energy interval, or equivalently to  $\lambda$ , of the photons is equal to:

$$\frac{\mathrm{d}^2 N}{\mathrm{d}x \mathrm{d}\lambda} = \frac{2\pi\alpha Z^2}{\lambda^2} \left( 1 - \frac{1}{\beta^2 n^2(\lambda)} \right). \tag{1.29}$$

This means that the greater part of Cherenkov photons are emitted in the ultraviolet range, because of the proportionality to  $1/\lambda^2$ .

Cherenkov detectors take advantage of this effect, detecting the light produced by charge particles. A large volume of transparent material, such as water, ice, or liquid scintillator, can be surrounded by lightsensitive detectors in order to capture the Cherenkov radiation. This technique is largely used in neutrino detection, since they cannot be detected directly: the charged lepton, yeilded in CC or NC interactions, is observed. From the light collected, it is possibile to reconstruct information on the

<sup>&</sup>lt;sup>2</sup>For this calculation, the convention c=1 is adopted.

interaction, such as the velocity of the charged particle, which is somehow related to the energy of the incident neutrino, or the position of the interaction vertex. If the charged lepton drop under the Cherenkov threshold, the light is emitted in the shape of a ring, which further data can be inferred from. Not every neutrino energy allows the production of a charged lepton<sup>3</sup>, but only MeV-scale neutrinos can be observed in a Cherenkov detector.

#### 1.2.2 Gadolinium neutron capture

#### to be improved.

Current multi-kiloton scale water Cherenkov detectors, like Super-Kamiokande (SK), have provided many clues in the experimental understanding of the neutrino, be it originated in solar, atmospheric, or accelerator reactions. However, in spite of the large lifetime of the experiment, some analyses are still limited by statistical uncertainty, and would benefit from increasing exposure. Other analyses suffer from background contamination, as in the case of the supernova relic neutrinos (SRN) search, and would benefit more from the development of new background suppression techniques. This hindrance can be overcome by studying the yield of neutrons in neutrino interactions, such as the *inverse beta decay* (the antineutrino CCQE scattering). It would allow a handle on antineutrinos rate, and possibly a method of background reduction for other studies.

Since neutrons are chargeless, they cannot interact with matter by means of the Coulomb force, which dominates the energy loss mechanisms for charged particles, described by the Bethe formula. Neutrons can interact with nuclei in various way, depending on the energy:

- elastic and inelastic scattering;
- transmutation;
- neutron activation;
- spallation reaction;
- neutron-induced fission;

As a result of the interaction, the neutron may either be absorbed, or change its energy and direction significantly. In this way the average energy of a neutron beam can be completely or partly reduced up to thermal energies, close to 0.025 eV. In this range of energy, the neutron presents a different and often much larger effective neutron absorption cross-section for a given nuclide, compared to, for instance, fast neutrons, hence thermalisation can result in a neutron activation process. This occurs when atomic nuclei capture free thermal neutrons, creating heavier nuclei, often in an excited state. The excited nucles decays almost instantaneously emitting usually gamma rays.

<sup>&</sup>lt;sup>3</sup>For instance, the CCQE process  $\bar{\nu}_e + p \to n + e^+$  has a energy threshold of 1.81 MeV and the interaction  $\nu_{\mu} + n \to p + \mu^-$  has the threshold of 110.16 MeV, because of the muon mass.

The neutron energy distribution is adopted to the Maxwellian distribution known for thermal motion. The time required by the thermalisation of neutrons follows an exponential, and the time constant is largely studied, [ref needed], amongst all the thermalisation in water. It was found that neutron thermalisation in water has a time constant of  $5\mu$ s [fujino, sumita, shiba]. Neutrons can be captured by either the hydrogen or the oxygen. Free neutron will capture on a hydrogen nucleus, releasing a 2.2 MeV gamma. In SK, for instance, this gamma results in about seven photo-electrons, and thus only detectable with  $\simeq 20\%$  efficiency.

Gadolinium-157 has the highest thermal neutron capture cross-section among any stable nuclides: 259,000 barns. Dissolving gadolinium compounds in water could considerably increase the neutron capture probability. The neutron in water thermalises quickly and can thus be captured by a Gd nucleus with a probability of 90 %. Upon capturing a neutron the Gd emits 3-4 gamma rays having a total energy of about 8 MeV. The time and spatial correlation of the positron and neutron capture events (20  $\mu$ s and 4 cm) can significantly reduce the backgrounds, and hence enhance the nu e signal events. Even moderately energetic neutrons ranging from tens to hundreds of MeV will quickly lose energy by collisions with free protons and oxygen nuclei in water. Once thermalised, the neutrons undergo radiative capture, combining with a nearby nucleus to produce a more tightly bound final state, with excess energy released in a gamma-ray ( ) cascade. Gd-doped water enhances the capture cross-section compared to pure water (49,000 barns compared with 0.3 barns on a free proton) and, since the cascade happens at higher energies (8 MeV vs 2.2 MeV), it produces enough optical light to be reliably detected in a large target volume.

#### 1.3 Neutrino Production

Numerous are the neutrino sources at the reach of neutrino experiments. Neutrinos are produced in CC interactions, which can happen in nuclear reaction, as for *solar* or *reactor* neutrinos, or in cosmic rays impacts with the Earth's atmosphere, conveying energetic *atmospheric* neutrinos.

Artificial neutrinos are also yielded in high-energy proton accelerators. Accelerator neutrino beams are fundamental instrumental discovery tools in particle physics, in that more control less variables are involved. Neutrino beams are derived from the decays of charged  $\pi$  and K mesons, which in turn are created from proton beams striking thick nuclear targets. The precise selection and manipulation of the  $\pi/K$  beam control the energy spectrum and type of neutrino beam.

The  $\pi^{\pm}$  mesons have a mass of 139.6 MeV and a mean lifetime of  $2.6 \times 10^{-8}$  s. The primary decay mode of a pion, with a branching fraction of 99.9877%, is a leptonic decay into a muon and a muon neutrino:

$$\pi^+ \to \mu^+ + \nu_{\mu}$$
 (1.30)

$$\pi^- \to \mu^- + \bar{\nu}_{\mu}$$
 (1.31)

The second most common decay mode of a pion, is the leptonic decay into an electron and the corresponding neutrino,  $\pi^{\pm} \to \nu_e + e$ . In spite of the considerable differences in the space momentum, this process is suppressed with respect to the muonic one. This effect is called *helicity suppression* and is due to the great mass of the muon ( $m_{\mu} = 105.658$  MeV) compared to the electron's ( $m_e = 0.510$  MeV); this results in a stronger helicity-chirality correspondence for the electron rather than for the muon. Given that the  $\pi$  mesons are spinless, neutrinos are left-handed, and antineutrinos are right-handed, the muonic channel is preferred because of spin and linear momentum preservation. The suppression of the electronic decay mode with respect to the muonic one is given approximately within radiative corrections by the ratio:

$$R_{\pi} = \left(\frac{m_e}{m_{\mu}}\right)^2 \left(\frac{m_{\pi}^2 - m_e^2}{m_{\pi}^2 - m_{\mu}^2}\right) = 1.283 \times 10^{-4} \tag{1.32}$$

The measured branching ratio of the electronic decay is indeed  $(1.23 \pm 0.02) \times 10^{-4}$ .

As far as the charged K meson is concerned, it mainly decays in a muon and its correspective neutrino, with a branching ratio of 63.55%:

$$K^+ \to \mu^+ + \nu_{\mu}$$
 (1.33)

$$K^- \to \mu^- + \bar{\nu}_{\mu}$$
 (1.34)

The second most frequent decay (20.66%) is the decay into two pions,  $K^{\pm} \to \pi^0 + \pi^{\pm}$ . Other decays have a branching ratio of 5% or less and are listed in table Tab. 1.1. On the contrary, the decays of the neutral kaon produce neutrino in few cases. Because of the oscillation phenomenon given by the mixing between  $K^0$  and  $\bar{K}^0$ , the neutral kaon has two manifestations, the short kaon  $K_S$  and the long kaon  $K_L$ , named after their lifetimes. While the K-short decays only in two pions  $(2\pi^0 \text{ or } \pi^+ + \pi^-)$ , the K-long has a wider variety of final state combination, all of them involving three particles. Among these, neutrinos are produced in the processes:

$$K_L^0 \to \pi^{\pm} + \mu^{\mp} + {\binom{-}{\nu}}_{\mu}$$
 (1.35)

$$K_L^0 \to \pi^{\pm} + e^{\mp} + {(-) \choose \nu}_e$$
 (1.36)

Neutrinos are also produced by the decay of muons. Muons are unstable elementary particles and decay via the weak interaction. The dominant decay mode, called *Michel decay*, is also the simplest possible: because lepton numbers must be conserved, one of the product neutrinos of muon decay must be a muonic neutrino and the other an electronic antineutrino, along with an electron, because of the

Tab. 1.1: Decay mode for a charged kaon,  $K^{\pm}$ , sorted by branching ration (in percent).

$\mu^{\pm} + {(-)\atop \nu}_{\mu}$	$65.55 \pm 0.11$
$\pi^{\pm} + \pi^0$	$20.66 \pm 0.08$
$\pi^+ + \pi^{\pm} + \pi^-$	$5.59 \pm 0.04$
$\pi^0 + e^{\pm} + {(-) \choose \nu}_e$	$5.07 \pm 0.04$
$\pi^0 + \mu^{\pm} + {(-) \choose \nu}_{\mu}$	$3.35 \pm 0.03$
$\pi^{\pm} + \pi^0 + \pi^0$	$1.76 \pm 0.02$

charge preservation. Vice versa, an antimuon decay produces the corresponding antiparticles. These two decays are:

$$\mu^- \to e^- + \bar{\nu}_e + \nu_\mu$$
 (1.37)

$$\mu^+ \to e^+ + \nu_e + \bar{\nu}_{\mu}$$
 (1.38)

The neutrino source provided by the muon decay, is more of a nuisance background, because of the long lifetime, which give rise to electronic component in neutrino spectrum. Usually a beam absorbed is located at the end of the decay region of an accelerator line, to stop the hadronic and muonic component of the beam, and only an almost pure neutrino beam pointing towards te

This is chapter 1.

## Chapter 2

This is chapter 2.

# Chapter 3

This is chapter 3.

## Appendix A

# Appendix 1

This is appendix 1.

## Appendix B

# Appendix 2

This is appendix 2.

## Appendix C

# Appendix 3

This is appendix 3.